AD NUMBER
ADB006333
LIMITATION CHANGES
TO: **Approved for public release; distribution is unlimited.**
FROM: **Distribution authorized to U.S. Gov't. agencies only; Test and Evaluation; 08 JUL 1975. Other requests shall be referred to Naval Electronics Laboratory Center, San Diego, CA 92152.**
AUTHORITY
USNELC ltr, 22 Apr 1976

NELC / TR 1956

NELC / TR 1956

MULTIFREQUENCY ARRAYS: DESIGN AND COST CONSIDERATIONS

J. H. Provencher, G. Vaughn,
D. Proctor, and J. E. Boyns

8 July 1975

Research and Development for period 3 March 1969 to 2 July 1975

Distribution limited to U.S. Government agencies only; test and evaluation; 8 July 1975. Other requests for this document must be referred to the Naval Electronics Laboratory Center, San Diego, California 92152

NAVAL ELECTRONICS LABORATORY CENTER
SAN DIEGO, CALIFORNIA 92152

UNCLASSIFIED

SECURITY CLASSIFICATION OF THIS PAGE (When Data Entered)

REPORT DOCUMENTATION PAGE

READ INSTRUCTIONS BEFORE COMPLETING FORM

1. REPORT NUMBER
NELC Technical Report 1956 (TR 1956)

2. GOVT ACCESSION NO.

3. RECIPIENT'S CATALOG NUMBER

4. TITLE (and Subtitle)
MULTIFREQUENCY ARRAYS: DESIGN AND COST CONSIDERATIONS

5. TYPE OF REPORT & PERIOD COVERED
Research and Development
3 March 1969 - 2 July 1975

6. PERFORMING ORG. REPORT NUMBER

7. AUTHOR(s)
J. H. Provencher, G. Vaughn, D. Proctor, and J. E. Boyns

8. CONTRACT OR GRANT NUMBER(s)

9. PERFORMING ORGANIZATION NAME AND ADDRESS
Naval Electronics Laboratory Center
San Diego, CA 92152

10. PROGRAM ELEMENT, PROJECT, TASK AREA & WORK UNIT NUMBERS
62751N, F12141, SF12141702
(NELC D210)

11. CONTROLLING OFFICE NAME AND ADDRESS
Naval Sea Systems Command
Washington, DC 20362

12. REPORT DATE
8 July 1975

13. NUMBER OF PAGES
44

14. MONITORING AGENCY NAME & ADDRESS (if different from Controlling Office)

15. SECURITY CLASS. (of this report)
UNCLASSIFIED

15a. DECLASSIFICATION/DOWNGRADING SCHEDULE

16. DISTRIBUTION STATEMENT (of this Report)
Distribution limited to U.S. Government agencies only; test and evaluation; 8 July 1975. Other requests for this document must be referred to Naval Electronics Laboratory Center.

17. DISTRIBUTION STATEMENT (of the abstract entered in Block 20, if different from Report)

18. SUPPLEMENTARY NOTES

19. KEY WORDS (Continue on reverse side if necessary and identify by block number)
Phased array
Multifrequency array
Cost analysis
Stripline slots
Frequency scanned array

20. ABSTRACT (Continue on reverse side if necessary and identify by block number)
This report describes several multiband antenna techniques and a method of cost analysis for array antennas. A concept is given which has potential to reduce overall array costs for large phased array systems by using component commonality to propagate several frequency bands. Techniques which can be used to reduce the cost, weight, and complexity of phased arrays are given, as well as potential applications for these techniques on small craft such as the hydrofoil.

DD FORM 1 JAN 73 1473 EDITION OF 1 NOV 65 IS OBSOLETE
S/N 0102-014-6601

UNCLASSIFIED

SECURITY CLASSIFICATION OF THIS PAGE (When Data Entered)

OBJECTIVE

Review multiband antenna techniques and a method of cost analysis for array antennas.

RESULTS

1. The cost of array antennas is not as expensive as it may appear as the antennas can perform several functions at different frequency bands.

2. Compact array antennas can be utilized where physical space is at a premium.

RECOMMENDATIONS

1. Perform a cost tradeoff versus performance to determine an optimum multiband array antenna for small, high-speed craft.

2. Perform a comparative cost analysis for the two band array to determine a cost figure of merit.

3. Analyze the dual band phase shifter to determine the minimum number of bits, path lengths, and impedance characteristics for the shared two frequency phase shifter.

4. Design and fabricate a two-band phase shifter and associated driver to determine the performance characteristics.

5. Design and fabricate a two-band radiating element to determine mode coupling, propagating characteristics, and impedance properties of a two-band element.

ADMINISTRATIVE INFORMATION

Work was performed as a portion of NELC Project D210, program element 62751N, under SF 12141702 as part of the Antenna Techniques Program by members of the Microwave Technology Division. This technical report has been prepared because it is believed that the information contained herein can be useful to other surveillance systems engineers and designers working in the field. The report was approved for publication 8 July 1975.

CONTENTS

ILLUSTRATIONS

ILLUSTRATIONS (Continued)

TABLES

INTRODUCTION

Array antennas have been thoroughly investigated during the past two decades and even though the techniques are well known and have been amply demonstrated, the use of arrays in operational systems has been minimal. The primary reason for this is the high cost of the array. Basically, the array must be cost competitive with the rotating reflector antennas which are currently used in the Fleet. All of the conventional arguments in favor of array use can be advanced, ie, improved data rate, agility, high gain, graceful degradation, etc, but these are all overshadowed by the high cost factor. What, then, is a practical solution to the problem? First, one must recognize that the array antenna is not a solution to all antenna problems of the Navy and in this respect, one must attack the problem by considering the major use of the array as used on a particular platform For example, an array for use on a large ship such as a carrier should not be lumped in a general "array" class with an array on a hydrofoil or one on a high-speed craft under the banner "arrays cost too much, we cannot afford them." Arrays are different and in the hydrofoil case, an array is a practical solution that could be cost competitive with one or more rotating type antennas. It is in this context that the cost considerations for phased arrays should be considered and not simply that "arrays are too expensive."

The preceding discussion presents two distinct array problems:

1) large, multielement, high gain, and high power arrays, which, to be cost competitive, must replace several rotating type systems to provide multifunction capability, and,

2) small, compact, lightweight, highly agile arrays to perform several functions over short ranges.

Both of these applications suggest some form of the multifrequency array* and will be discussed in this report in addition to cost analysis results. Multifrequency array studies conducted at NELC** in recent years have shown their feasibility, and have also demonstrated several configurations, one of which is shown in figure 1.

From previous studies in single frequency arrays, the control of the required phase shifts to steer the beam is most critical. In addition, phase errors result from tolerance errors in the component chain, and introduce losses in power and beam pointing angle deviations. These practical considerations will be discussed.

The cost of the phased array is dependent upon many factors.

---

*US Patent 3,193,830, J. H. Provencher, Multifrequency Dual Ridge Slot Antenna, 6 July 1965

**US Patent 3,623,111, J. H. Provencher, et al, Multiaperture Radiating Array Antenna, 23 Nov 1974

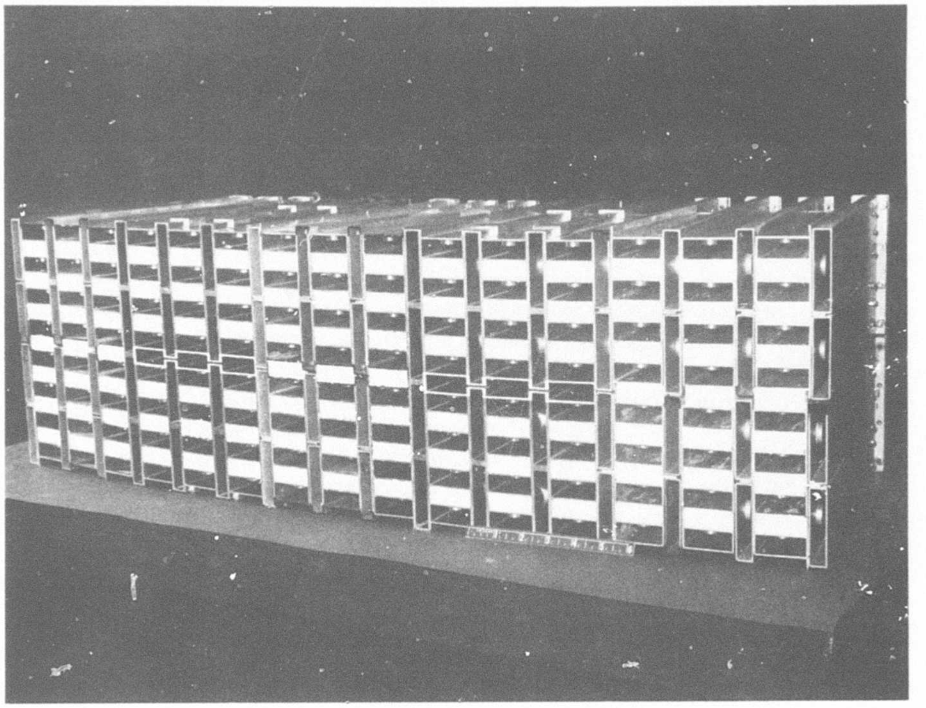

Figure 1. Three-band multifrequency array – waveguide.

PART I

1.1 BACKGROUND

Phased array antenna techniques show promise of providing high system reliability, high beam agility, flexible power control, beam shaping and stabilization, multiple-target capability, etc. The application of these highly desirable antenna qualities is dependent upon either low-cost array components or multiple use of components. The adaptation of these antennas for widespread Fleet use has been awaiting the development of a technology that would provide complex, reliable and efficient circuits of relatively small size, high reproducibility and low cost. Microwave integrated circuit (MIC) techniques offer these features. This technology is now developing rapidly, and could become cost effective. The techniques are being extended into the 20-60 GHz frequency region and for the short range, high resolution application such as the small craft, the frequencies appear attractive. This section describes a concept which makes use of a single phase shifter and radiating element to propagate several frequencies in a dual frequency array. The next section describes particular techniques for possible use on the small array application as well as for the pencil beam type of array.

1.2 THE CONCEPT

Traditionally, the phased array antenna consists of many individual radiating elements which are excited through a corporate feed system to form a beam, and then steered in many planes by means of a phase shifter at each element. If N_a is the number of elements in the azimuth plane and N_e is the number of elements in the elevation then the total number, N, of phase shifters required is

$$N = N_e N_a, \text{ and} \tag{1}$$

if a pencil beam is required, then $N_a = N_e$ and

$$N = N_e^2 \tag{2}$$

Since the phase shifter and its associated driver account for about one half of the total array cost, it is evident that a reduction in the number of phase shifters is necessary for any significant cost reduction.

The approach to be described makes use of a single phase shifter per element, while it allows several frequency bands to be used in the device to reduce the number of antennas required to perform several different functions and provides a "clear" field of view for each beam.

1.3 THE ARRAY: BASIS

There are several restrictions which must be placed on the array to ensure that the basic array equations are satisfied for the frequency bands of interest. These restrictions, however, do not place any severe limitation on the array performance, since in actual practice these restrictions are present. One requirement is that the operating frequencies selected are approximate multiples of each other, for example, 1.0 GHz and 3.0 GHz. Another requirement is that the array element spacings selected satisfy the equation for scanning at the highest operating frequency, ie,(for a single band linear array),

$$\psi = \left(\frac{2\pi}{\lambda}\, d_h \sin\theta \pm \delta\right) M \tag{3}$$

ψ is the total phase across the array, $2\pi/\lambda$ is the propagation constant, and M is the total number of elements. The phase increment between elements, (δ), is required to position the beam at an angle θ as shown in figure 2. The element spacing, d_h, is the physical spacing of the radiating elements at the highest operating frequency.

From equation (3), then, it follows that for a dual frequency array with the frequencies a multiple of each other, the following equations must be satisfied; ie,

$$\left.\begin{cases} \psi^{(1)} = \dfrac{2\pi}{\lambda_1}\, d_{h_1} \sin\theta_1 \pm \delta_1 \\[2ex] \psi^{(2)} = \dfrac{2\pi}{\lambda_2}\, d_{h_2} \sin\theta_2 \pm \delta_2 \end{cases}\right\} \quad f_2 > f_1 \tag{4}$$

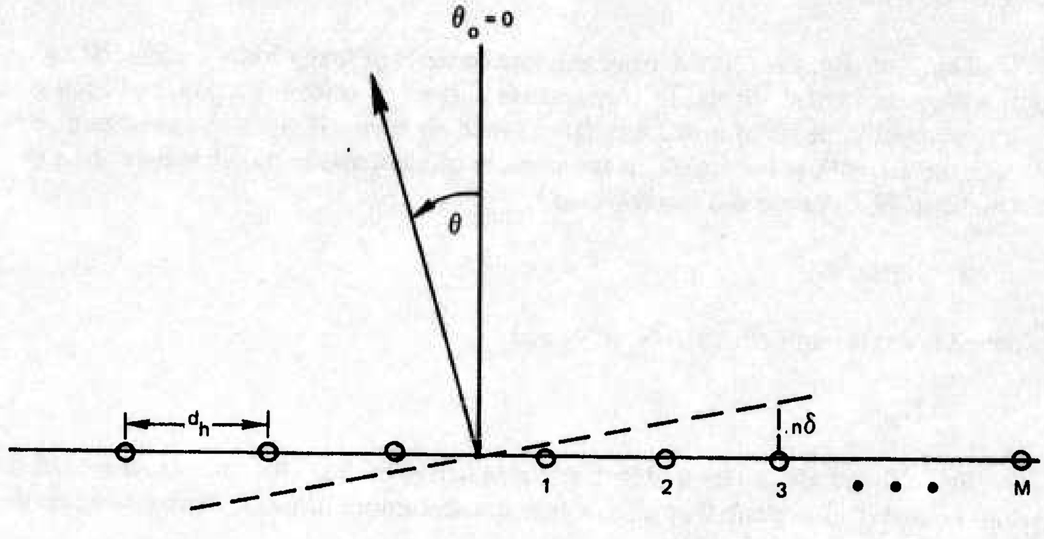

Figure 2. Array definition.

In order to suppress grating lobes, the maximum allowable element spacing is $0.59\lambda_2$ to scan the beam to ±45°. Thus,

$$\left\{\begin{array}{l}\delta_2 = k_2 d_2 \sin\theta_2 \\ \delta_1 = k_1 d_1 \sin\theta_1\end{array}\right\} , \qquad k_i = \frac{2\pi}{\lambda i} , \ i = 1, 2. \tag{5}$$

Now, if $f_2 = 3\,f_1$, (5) becomes

$$\left\{\begin{array}{l}\delta_2 = k_2 d_2 \sin\theta_2 \\ \delta_1 = (1/3)\,k_2 d_1 \sin\theta_1\end{array}\right\} , \qquad f_2 > f_1 \tag{6}$$

and if $d_1 = 2d_2$, then

$$\left\{\begin{array}{l}\delta_2 = k_2 \dfrac{d_1}{2} \sin\theta_2 \\ \delta_1 = (1/3)\,k_2 d_1 \sin\theta_1\end{array}\right\} . \tag{7}$$

Therefore:

$$\delta_1 = (2/3)\,\delta_2 \frac{\sin\theta_1}{\sin\theta_2} , \qquad f_2 > f_1 \tag{8}$$

From this expression, the allowable limits of a dual band array can be determined.

1.4 THE PHASE SHIFTER

The switched-line phase shifter bit consists of two single-pole double-throw (SPDT) switches and two different lengths of transmission line. The phase shift, ξ, is given by the difference in the electrical lengths of the lines $(L - L')$

$$\xi = k\,(L - L') \text{ radians.} \tag{9}$$

Since this device is a linear function of frequency, it can be used by two or more frequencies which are multiples of each other and as shown schematically in figure 3.

Combinations of the various bits of the phase shifter result in a phase increment, δ, which is applied to the radiating element. When the path lengths $(L - L')$ are chosen to be

$$\frac{2\pi}{2^{\eta}}\ , \quad n = 0, 1, 2, \ldots \eta \tag{10}$$

at the lower operating frequency, then the path lengths become

$$\frac{2\pi m}{2^{\eta}}\ , \quad n = 0, 1, 2, \ldots \eta \tag{11}$$

at a higher frequency. The number of phase shifter bits is η, and m is the ratio of the higher to lower frequencies. Selection of the number of bits for the optimum two frequency array

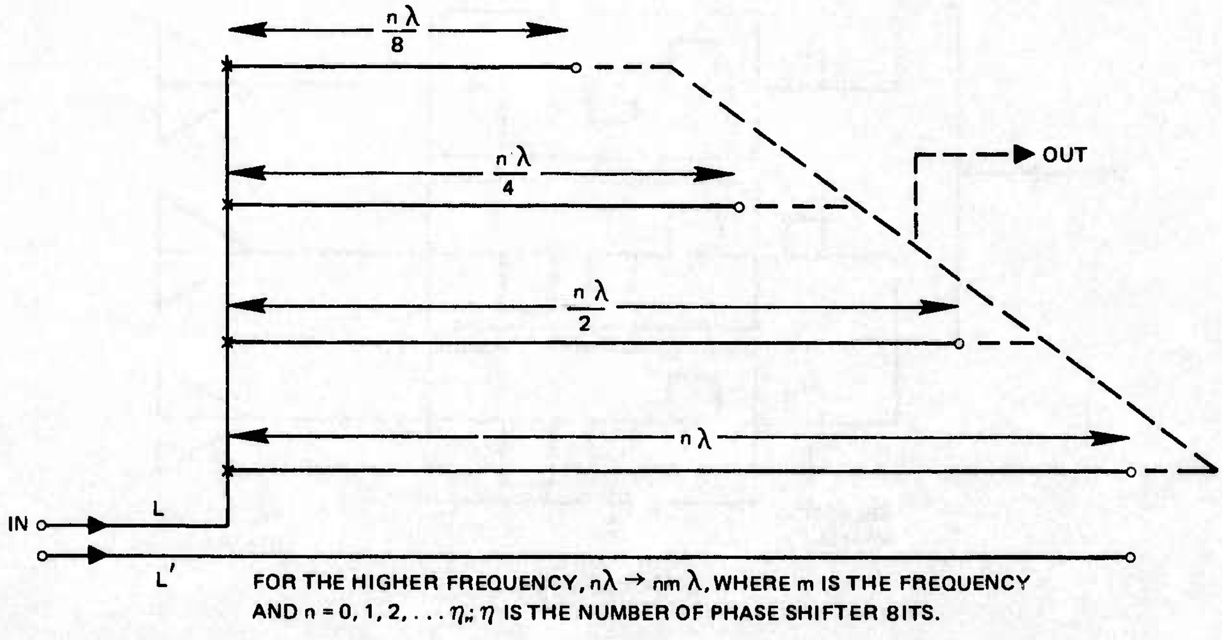

Figure 3. Switched-line phase shifter for a two-frequency ratio.

is a compromise which must be made after considering scan angle and effects due to phase quantization losses.

For example, when $\eta = 3$, at the lower frequency, n = 0, 1, 2, 3, and

$$\frac{2\pi}{2^{\eta}} = 2\pi, \pi, \frac{\pi}{2}, \frac{\pi}{4}.$$

Then (L – L′) at the higher frequency becomes (for m = 3)

$$\frac{2\pi \cdot 3}{2^{\eta}} = 6\pi, \frac{6\pi}{2}, \frac{6\pi}{4}, \frac{6\pi}{8}$$

or

$$3\left(2\pi, \pi, \frac{\pi}{2}, \frac{\pi}{4}\right).$$

Thus, it can be seen that the same bits are present in both cases except for a common factor. This factor can be changed by the addition of the selector switch shown in figure 4.

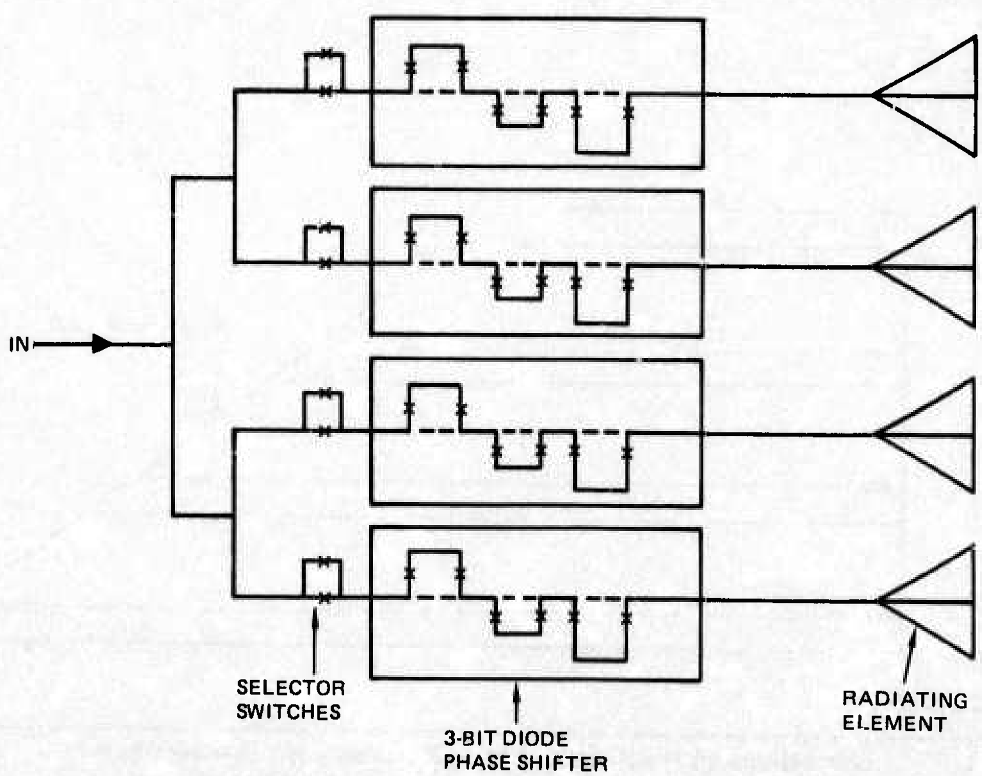

Figure 4. Dual frequency array concept.

Another type, the periodically-loaded line bit, consists of two equal susceptances spaced 1/4 wavelength apart loading a line of admittance Y_1. The susceptances are either of two states, $\pm j\beta$, as the diodes are switched. The chase shift is related to these parameters by

$$Y_1 = Y_0 \sec \frac{(\Delta\theta)}{2} \text{ and } \beta = Y_0 \tan \frac{(\Delta\theta)}{2}$$

where Y_0 is the admittance of the lines external to the bit.

In the forward bias condition, the diodes shunt the stubs. L is less than 1/4 wavelength and for small phase shifts is given by

$$L_1 = \frac{\lambda}{4}\left(1 - \frac{\beta}{\gamma}\frac{2}{\pi}\right).$$

When reverse biased, the electrical length of the stubs is greater than 3/4 wavelength and for small phase shifts is given by

$$L_2 = \frac{\lambda}{4}\left(3 + \frac{\beta}{\gamma}\frac{2}{\pi}\right)$$

Thus, in the forward bias, the susceptance is inductive and in reverse bias it is capacitive. The phase is delayed in reverse bias. Similar expressions can be derived when L = 3/4 wavelength. Combinations of these bits can be used in the phase shifter in addition to the bit previously described.

Examination of equation (4) reveals the relationship between the element spacing, d, the beam pointing angle, θ, and the phase increment, δ, required to position the beam in a given direction. Consider a two-frequency band array for $f_1 = 1.0$ GHz and $f_2 = 3.0$ GHz, when $\theta_1 = \theta_2$. Table 1 gives the required phase increments for each frequency at several scan angles when $d_1 = 12$ cm, or when $0.4\ \lambda_1$ and $d_2 = d_1/2 = 6$ cm or $0.6\ \lambda_2$. From equation (8), when $\sin\theta_1 = \sin\theta_2$, then

$$\delta_1 = \frac{2}{3}\,\delta_2$$

For each of the two center frequencies, there results at each bit in the phasor,

$$\Delta^{(1)}\Psi = k_1 (L - L)$$

$$\Delta^{(2)}\Psi = k_2 (L - L') \text{ radians.}$$

When $\lambda_1 = 3\lambda_2$ and m = 4 for a 16 element array and for a scan angle of 45°, the required increments are given in table 2. The phase shift error due to the truncation is ±10.7° for f_1 and ±11.1° for f_2.

TABLE 1. PHASE INCREMENTS FOR VARIOUS SCAN ANGLES.

ANGLE	PHASE INCREMENT		PHASE SETTING	
$\theta_1 = \theta_2$	1	2	f_1	f_2
0.0	0.0	0.0	0.0	0.0
5.0	12.5	18.8	22.5	22.5
10.0	25.0	37.5	45.0	45.0
15.0	37.3	55.9	45.0	45.0
30.0	72.0	108.0	67.5	112.5
45.0	101.8	152.7	112.5	157.5

TABLE 2. PHASE SETTINGS AND ERRORS
FOR 16 ELEMENT ARRAY.

Element Number	0	1	2	3	4	5	6	7	8
$\Psi_1 = M\delta_1$ Degrees	0	101.8	203.6	305.4	407.2	509.0	610.8	712.6	814.4
Phasor Setting (f_1) (4 bits) Degrees	0	112.5	202.5	315.0	45.0	157.5	247.5	337.5	90.0
Error Degrees	0	+10.7	−1.1	+10.2	−1.6	+9.1	+7.3	−7.5	+6.2
$\Psi_2 = M\delta_2$ Degrees	0	152.7	305.4	458.1	610.8	763.5	916.2	1068.9	1221.6
Phasor Setting (f_2) (4 bits) Degrees	0	157.5	315.0	90.0	247.5	45.0	202.5	337.5	135.0
Error Degrees	0	+4.8	+9.6	−8.1	−3.3	+1.5	+6.3	−11.4	−6.6

1.5 THE ARRAY: PRACTICAL CONSIDERATIONS

In order to implement a dual frequency array, some practical problems must be considered in addition to the basic assumption that the phase shifters and elements are feasible. The gain, beam pointing angle, and side-lobe level are affected by the errors due to fabrication tolerances, truncation of the phase shifters, and variations in the applied amplitude and phase excitation.

The gain of each array is given by the expression

$$G = \Lambda \frac{\left| \sum_{i=1}^{M} (G_{ei})\, 1/2\, A_i e^{j\delta_i} \right|}{\sum_{i=1}^{N} A_i 2}, \quad i = 1, 2, \ldots M \tag{12}$$

where

Λ = total loss of array

G_{ei} = power gain of i^{th} element

δ_i = phase of i^{th} element

A_i = relative voltage of i^{th} element

M = total number of elements

Assuming the δ_i includes only a linear beam steering element phase, then the other phase effects are included in the series

$$\sum \Lambda_Q + \Lambda_\delta + \Lambda_f + \Lambda_S + \Lambda_R \tag{13}$$

where

Λ_Q = loss due to phase quantization

Λ_δ = loss due to rms phase errors

Λ_f = loss due to using same phasing for all frequencies

Λ_S = scan loss of element pattern

Λ_R = loss due to VSWR of array element

The overall gain then becomes

$$G = \Lambda\,(\mathrm{dB}) + G_e + 10 \log_{10} M \tag{14}$$

1.5.1 LOSSES

The total loss factor as given includes several phase terms

$$\Lambda = \Lambda_Q = \Lambda_\delta + \Lambda_f \tag{15}$$

Phase shift quantization results when using digital phase shifters; this loss is dependent upon the array scan angle. At boresight when the required phase shift is equal to the minimum bit size, the loss is zero. When the phase increment between elements is equal to one half the minimum bit size, the quantization loss is maximum. The reduction in gain due to phase quantization, ΔG_Q is

$$G_0 = 1 - \frac{\pi^2}{(6)\,(2^2\eta)} \tag{16}$$

A three-bit phase shifter yields a quantization loss on the order of 0.22 dB.

The RMS phase error, ϵ, is due to errors in various components of the array and is minimized by placing realistic tolerances on each component. Since the radiating elements and phase shifters form an integral part of the array concept, the effect of the phase shift errors of these components on beam pointing angle must be considered. When the total phase is small (less than 15°) the RMS phase error loss factor is

$$\Lambda_\phi = e^{-[k\epsilon]^2} \tag{17}$$

This loss, due to using discrete phase increments, results from the fact that the beam pointing direction is changed when the frequency is changed. The beam pointing angle is independent of frequency only when steering is accomplished by use of delay lines. For systems requiring a wide bandwidth, examination of equation (4) reveals that

$$\frac{\sin\theta_1}{\sin\theta_2} = \frac{f_1}{f_2} \quad . \tag{18}$$

This expression is maximum when the scan angle is maximum. Hence, for narrow-beam arrays this condition results in a loss of signal when wide-band signals are used unless true time delay units are used to reduce the scan loss. In a multifrequency array, where two frequencies use the same line lengths in the phase shifter, a compromise between bandwidth, scan loss, and line length must be made to avoid large scan losses.

1.5.2 PHASE ERROR EFFECTS

The finite errors in each of the components, coupled with the errors due to fabrication usually affect the radiation pattern and result in changes in the beam pointing angle and pattern side-lobe level.

A considerable change in side-lobe level is produced as a result of a maximum inter-element phase deviation as small as 1.5° when the array side-lobe level has been designed

for −33 dB and −40 dB. An additional increase in the phase deviation to 3° and 6° does not produce a proportionate increase in the near-side-lobe level when the number of elements is on the order of 50 as shown in figure 5. As the number of elements is increased, however, a maximum phase deviation of 3° yields a considerable increase in side-lobe level. In addition, the far-out side lobes increase progressively with an increase in the maximum phase deviation.

The array with a −33 dB Taylor distribution suffers slightly less side-lobe deterioration due to phase errors than does the Tchebyscheff distribution. For the lobes within 30° of broadside, however, the patterns resulting from the two distributions with the same errors assumed are similar (fig 5). Figure 6 shows the effects of phase errors as the beam is scanned to 19°. For applications requiring omnidirectional elements and low-side-lobes for far-out angles, stringent control of the phase distribution is required.

1.5.3 ERROR ANALYSIS

The determination of the effect of phase shift errors in the various components is primarily a statistical problem and, under certain assumptions, can give some indication of the effects on the array performance.

Considering the problem of a radiating element and its phase shifter connected in series as a portion of an array module and as shown in figure 7, the following assumptions are made:

1. The phase shift of the various elements is uniformly distributed over the range of ±a degrees, with the variance of $\sigma_e^2 = a^2/3$
2. The phase shift of the various phase shifters is uniformly distributed over the range ±b degrees with a variance of $\sigma_a = b^2/3$
3. The phase shift of any element or phase shifter is statistically independent of all other phase shifters and elements.

The third assumption indicates that there is no interaction between adjacent elements. For closely spaced elements, at the lower frequency, this assumption may not be entirely valid.

The phase shift of each element-phase shifter combination is obtained by a convolution using assumptions 1 and 2 where a > b and the variance is

$$\sigma_s = \frac{a^2 + b^2}{3} \tag{19}$$

The output signal of the i^{th} single combination is

$$v_i(t) = A_i \cos(\omega t + \Delta_i) \tag{20}$$

where

A_i = amplitude of i^{th} element

ω = radian frequency

Δ = the phase error resulting from element and phase shifter.

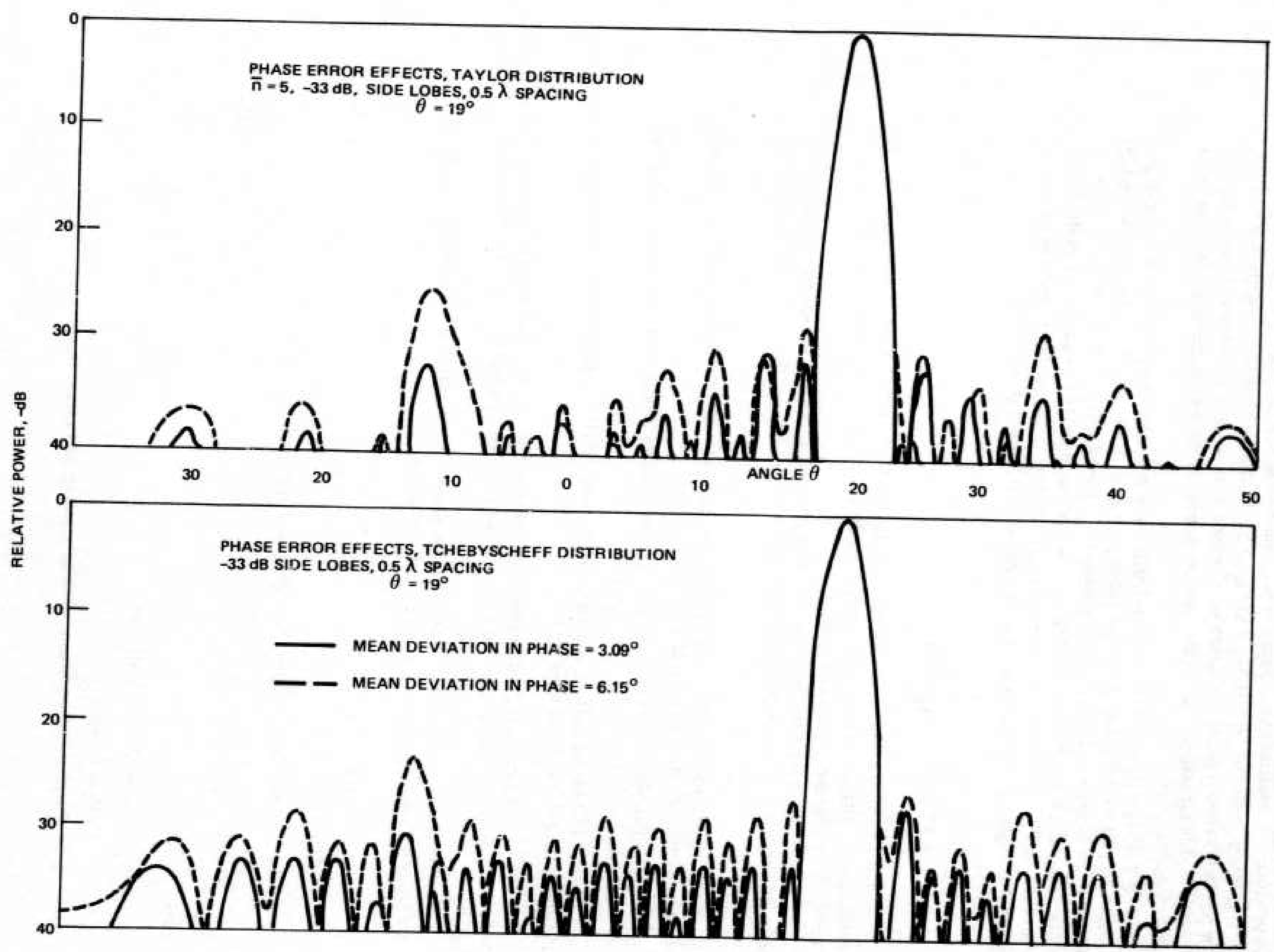

Figure 5. Phase error effects on side-lobe level.

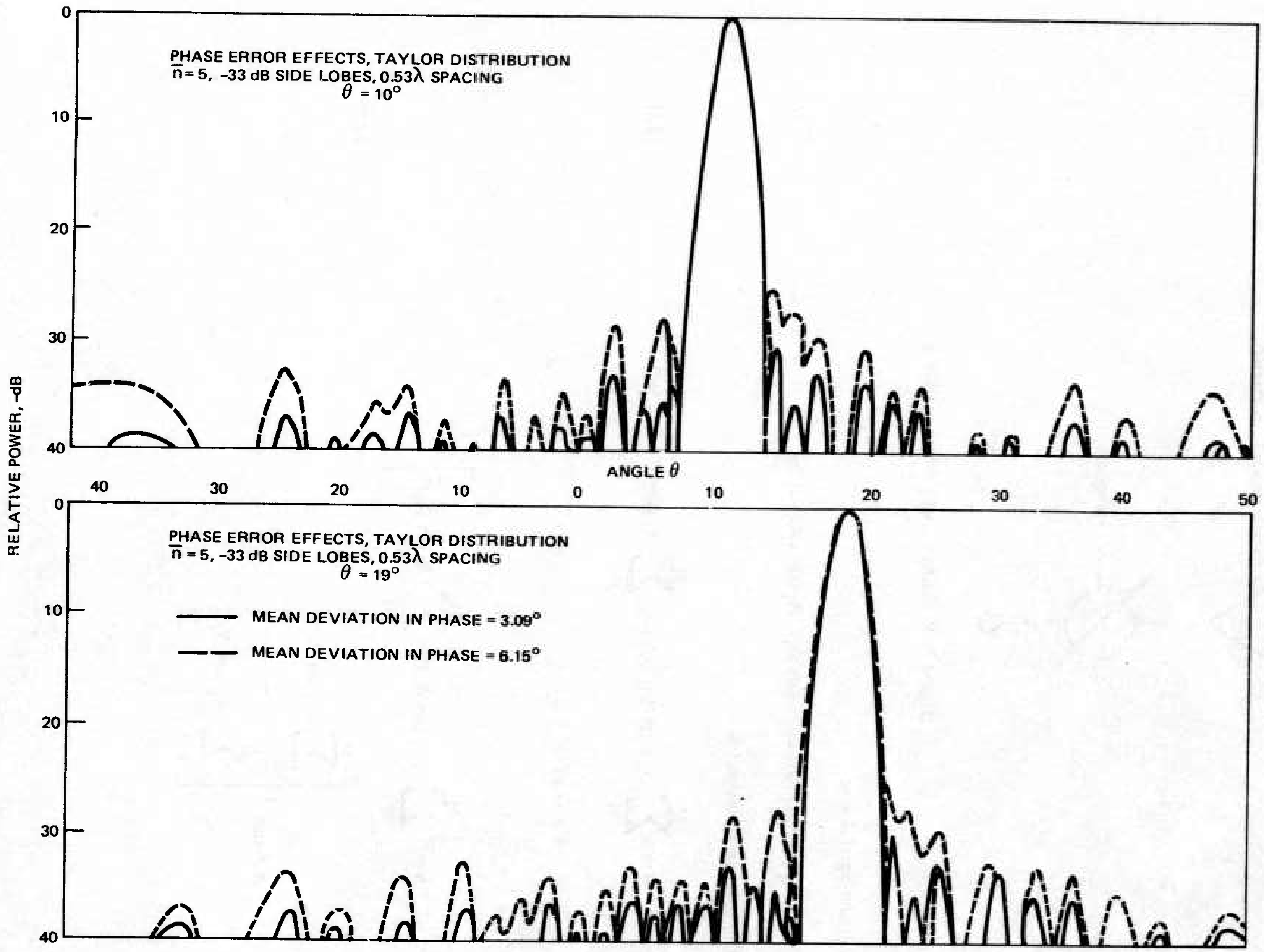

Figure 6. Phase error effects on scan angle pattern.

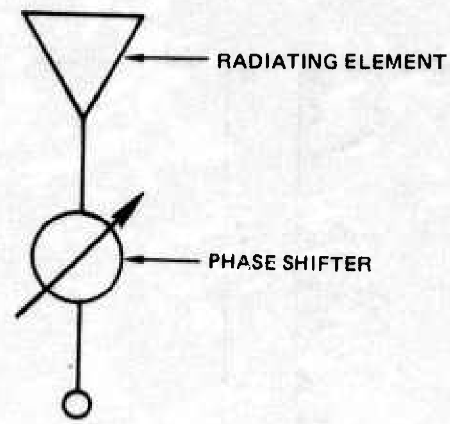

Figure 7. Radiating element and phase shifter.

Expanding v(t) gives

$$v_i\,(t) = A_i\,(\cos\omega t)\,(\cos\Delta_i) - A_i\,(\sin\omega t)\sin\Delta_i \tag{21}$$

The total array output is

$$\begin{aligned} v(t) &= \sum_{i=1}^{M} A_i\,(\cos\Delta_i)\cos\omega t - \sum_{i=1}^{M} A_i\,(\sin\Delta_i)\sin\omega t \\ &= A\cos(\omega t + \Delta) \end{aligned} \tag{22}$$

where

$$\begin{aligned} A &= \left[\sum_{i=1}^{M} (A_i\cos\Delta_i)^2 + \sum_{i=1}^{M} (A_i\sin\Delta_i)^2\right]^{1/2} \\ \Delta &= \tan^{-1}\left[\frac{\displaystyle\sum_{i=i}^{M} A_i\sin\Delta_i}{\displaystyle\sum_{i=1}^{M} A_i\cos\Delta_i}\right] \end{aligned} \tag{23}$$

When the element and phase shifter tolerances, a and b, are small and the amplitudes A_i are nearly equal as in large element arrays, then Δ becomes

$$\Delta \simeq \Delta' = \frac{\sum_{i=1}^{M} A_i \Delta_i}{\sum_{i=1}^{M} A_i} \tag{24}$$

From the practical standpoint, Δ has a Gaussian distribution with a variance

$$(\sigma')^2 = \frac{\left(\sum_{i=1}^{M} A_i^2\right)}{\left(\sum_{i=1}^{M} A_i\right)^2} \cdot \sigma_i^2 \tag{25}$$

$$= \frac{\left(\sum_{i=1}^{M} A_i^2\right)}{\left(\sum_{i=1}^{M} A_i\right)^2} \cdot \left(\frac{a^2 + b^2}{3}\right) \tag{26}$$

Hence, 68% of all elements should have a phase error Δ of magnitude less than σ. When the sum of the tolerances exceeds 15°, then the approximations are no longer valid. It is therefore essential that each component tolerance be held to the absolute minimum in the module.

In the multifrequency array, the tolerances must be such that the pattern characteristics for two or more frequency bands need to be satisfied. When the frequencies are in a 3:1 ratio, the component tolerances placed on the lower frequency components could have adverse effects on the performance at the higher frequency. Since the tolerance variations appear as phase shifts, they can be minimized by reprogramming the high-band phase shifters. Computer simulation can be used to determine the proper phase settings after the errors have been calculated. The allowable component combination tolerance to satisfy both frequency bands must be determined early in the array design.

PART II

2.1 INTRODUCTION

This section summarizes the results of an investigation to determine the feasibility of constructing light-weight scanning array antennas with the following characteristics:

a) from broadside azimuth scan

b) limited elevation scan

c) pencil beams

d) 30 dB sidelobes

Basic array configurations have been examined to satisfy these requirements. Using a single rf power source is one approach to feed all arrays; another is the possibility of using distributed rf power sources or amplifiers at each element (or for each column of elements). This report considers the first approach but does not preclude use of the other. Since significant costs in terms of weight complexity must be paid in order to achieve wide-angle characteristics, usually a slightly less rigid scan angle and/or beamwidth characteristics will allow practical tradeoffs.

Much effort has been devoted to developing phased array antennas with distributed rf sources or amplifiers (for example, the MERA, RASSR, and MAIR programs [22]). This work has been spurred in part by the need to use many low-power solid-state sources to achieve the required power levels, and in part by the reliability of many separate solid-state sources. Another advantage is that all the rf signal conditioning (power dividing and phase-shifting) can be done at low-power levels using lossy, but compact and lightweight, microwave integrated circuit techniques since final amplification can be done just before transmission. Distributed rf systems are currently complex and too costly to develop. Therefore, even though the production costs can be fairly low due to printed circuit and MIC techniques, many thousands of units must be produced to achieve a low cost per module. Since a high radiated power is not required for the small craft application and only a relatively small number of modules are required for each antenna, it appears that a single tube approach is desirable.

When an array is fed by a single, central power source, a key consideration is minimum power loss in the distribution and phasing network. Stripline is both relatively low loss and lightweight and is a preferred transmission line. MIC techniques are more lossy than waveguide but for the short ranges they can be an acceptable solution, especially where weight and space are critical. Various feed structures will be discussed and the parameters of a typical example will be summarized.

The use of the stripline techniques for multifrequency arrays that has been examined offers attractive, low cost, lightweight antenna approaches for both small craft and large ships. For small craft (and short range targets), the frequencies above 10 GHz could be used in a multifrequency array. This report discusses the array for larger ships and longer ranges, however, the techniques are also applicable for the smaller craft.

2.2 LIGHTWEIGHT ANTENNAS

One antenna examined was a planar phased array of slots in stripline. The elements have to be staggered so that the column spacing eliminates grating lobes. Figure 8 is an overview of the array and its feed.

Typically, to achieve a 6° beamwidth with 30 dB sidelobes, each column has 15 elements with a spacing of 0.934 or 1.10 inches. The center-to-center horizontal spacing is 0.52λ or 0.61 inch.

Three cases considered were:

(1) 24 elements per row

(2) 32 elements per row

(3) 48 elements per row.

The resulting properties of these three cases are summarized in table 3.

Each element in a column is fed in series (fig 9) and each column is fed by resonant coupling-slots between the power divider board and the radiating board for frequency scan. Each board has identical resonant slots. These slots are aligned so that the energy is coupled from the center conductor of the power divider board to the center conductor of the radiating board.

This basic stripline array structure can be used with several different feed techniques to provide limited elevation scan while maintaining its lightweight characteristics. Two of these techniques, the hybrid matrix and frequency scan, are discussed.

2.2.1 HYBRID MATRIX

For the hybrid matrix case, the slots in each array are separated by mode suppressing rivets or eyelets (fig 10) to form a stripline cavity into which a probe is inserted from the rear to provide an input from the matrix for amplitude and phase control. Multiport hybrid matrices using 8 and 16 ports have been fabricated using alumina substrates. These devices can be used to provide a limited elevation scan capability when used as a linear element in a planar array. Sum and difference beams can be achieved without additional complexity.

2.2.2 FREQUENCY SCAN

A frequency scanned planar array using the radiating structure described can be constructed in one piece of stripline (fig 11). This technique is low cost and lightweight

TABLE 3. PARAMETERS OF THE THREE-PHASED ARRAYS UNDER CONSIDERATION.

No. Rows	Height (in)	No Cols	Width (in)	Weight Radiating Board	Horizontal Beamwidth 0°	±45°	±60°	Directivity 0°	±60°
15	16.9	24	15.1	1.24 lb	6.1°	8.6°	12.2°	33.5dB	30.5dB
15	16.9	32	20.0	1.64 lb	4.6°	6.5°	9.2°	34.7dB	31.7dB
15	16.9	48	29.9	2.54 lb	3.05°	4.3°	6.1°	36.5dB	33.5dB

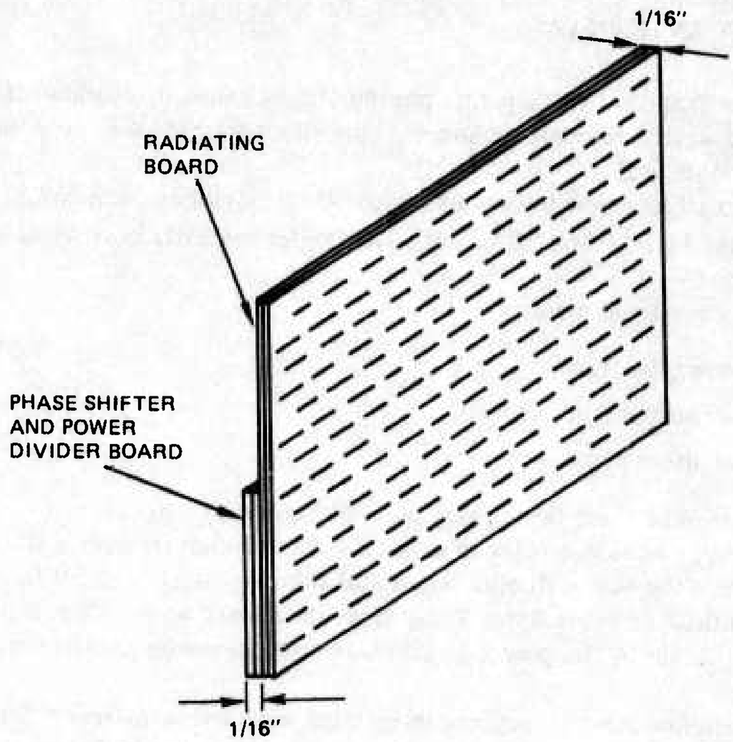

Figure 8. Staggered slot antenna board.

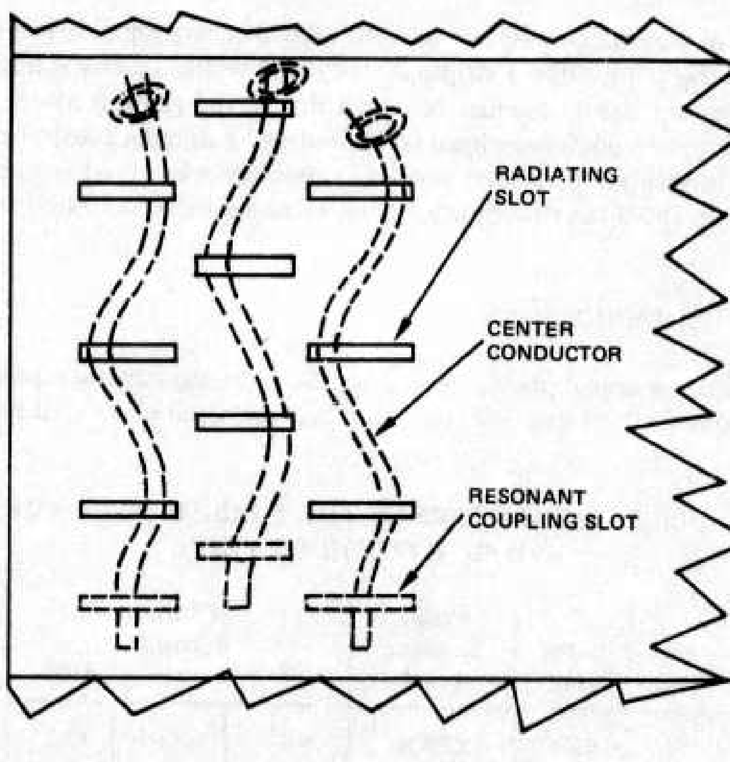

Figure 9. Details of array face.

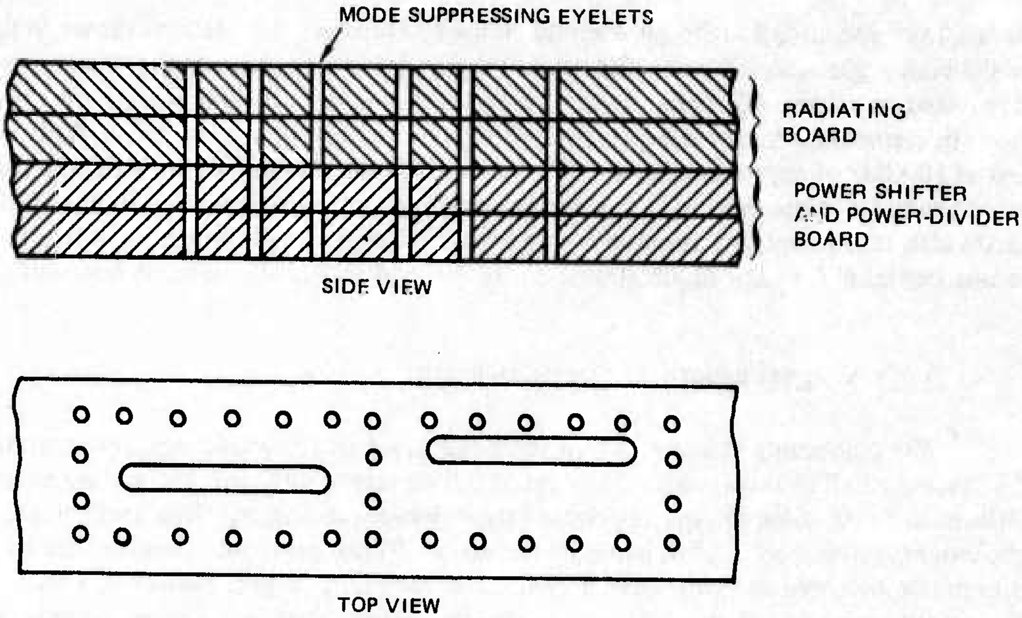

Figure 10. Stripline slot details.

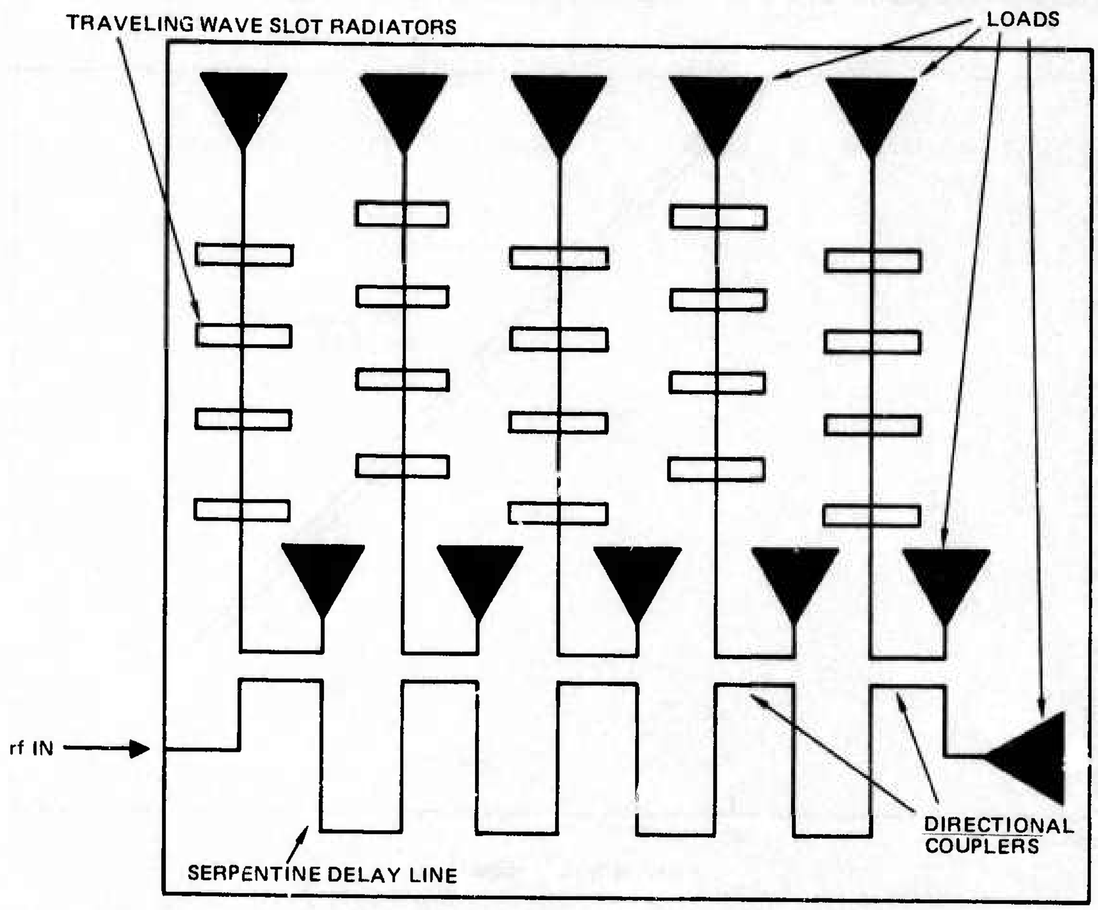

Figure 11. Typical single board frequency scan array.

since all printed circuit techniques would be used. However, calculations shown in figure 12 of the scan angle achievable as a function of delay line length indicate that a wide bandwidth is required to achieve 60° scan. Figure 12 shows that with 100 guide wavelengths between azimuth elements, a 90 Mc band is required to achieve ±60° scan at 10 GHz. With a typical loss at 10 GHz of approximately 0.025 dB/λ for 50 ohm line in 0.62 inch thick stripline, it is not practical to use more than 5 wavelengths delay between elements. Hence, an 18% bandwidth is required to achieve this scan angle. While realizing that this bandwidth may be unacceptable for some applications, it must be considered as a possible trade-off.

2.2.3 MULTIFREQUENCY TECHNIQUES

The combining of several elements in the same aperture area requires restriction of the spacing of all elements to a maximum of 0.6 wavelength (to prevent grating lobes) while at the same time the spacing chosen must prevent supergain. This limits the choice of elements to be used in both bands of the array. Flush waveguide elements can be used but are cumbersome and expensive in the lower frequency ranges. However, a flush mounted element such as a radiating slot in a metal sheet or in stripline is a more suitable choice to reduce weight and cost. The restriction in physical antenna space between the elements rules out the use of inclined or shunt slots.

Strip transmission line (commonly called stripline), consists of a flat conducting strip between the parallel to conducting ground planes as shown in figure 13. The stripline

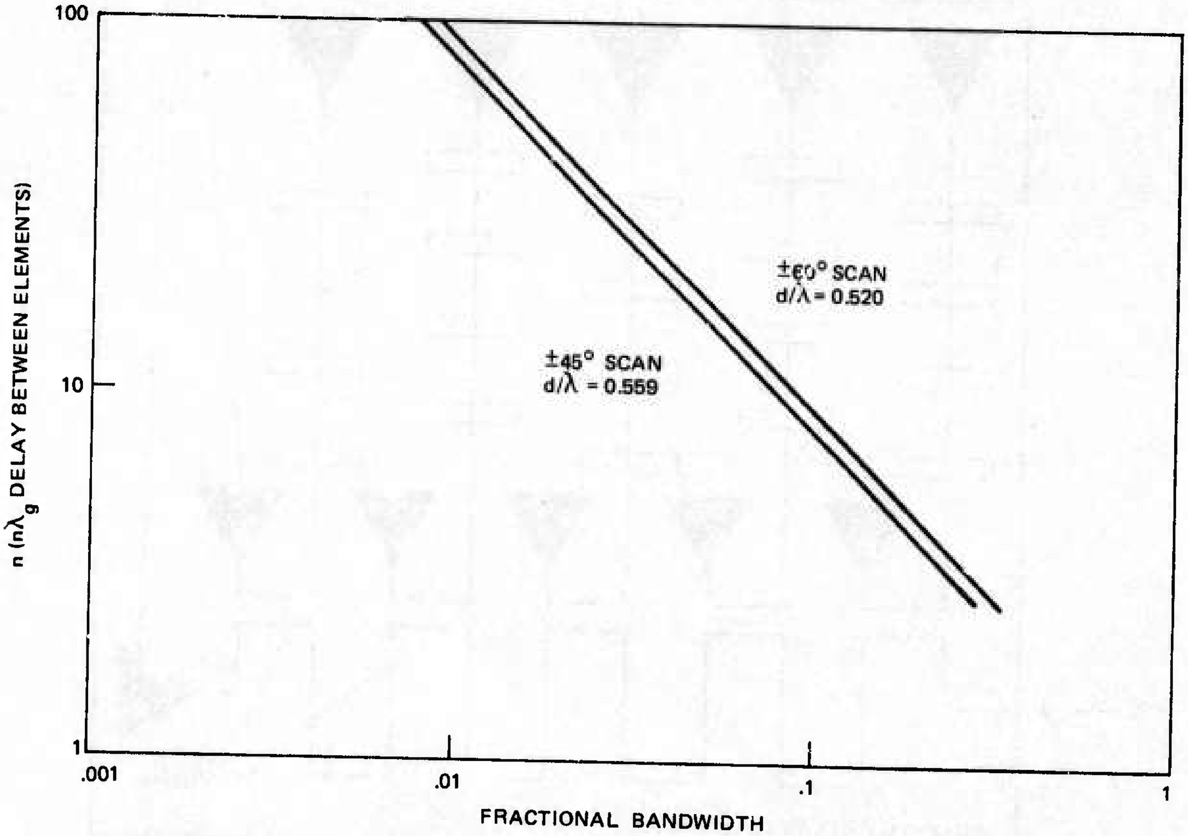

Figure 12. Bandwidth required to achieve ±45° or ±60° scan as a function of the delay between columns.

circuit is constructed by printing the conducting strip on one side of a section of the copper clad dielectric board. The radiating slot is etched on the opposite side of the same board. The board is combined with a similar one, which has had the copper removed from one side, to form the finished stripline sandwich. The two boards are thermally bonded and metal screws are inserted to short the ground planes together to prevent the generation of spurious and higher order modes. When the conducting strip is small compared to the ground planes, the electric field is almost entirely confined in the dielectric and the mode propagated is the TEM mode.

Typical D-band elements are cavity-backed radiating slots in stripline.* A slot cut in an infinitely large metal sheet or in a stripline will radiate efficiently when properly excited. Since stripline is a balanced circuit supporting the TEM mode, the slots must be cut in both ground planes to prevent unbalance. However, both sides would then radiate. To confine radiation to one side, it is necessary to enclose one slot in a cavity as shown in figure 14. The cavity is made one-quarter wavelength long and this approximately doubles the slot impedance. The sides of the cavity are left open to preserve the TEM mode. When the slot is filled with a dielectric, as in this case, the slot length is effectively increased. The increase in slot length must be taken into consideration when determining the resonant slot length.

To accommodate F-band elements, the boards are first prepared by punching 1.410 X 0.900 inch holes. The rubylith overlay is then fitted between the holes and the boards properly etched. The two halves of the stripline are assembled with an interleaving of HZ-1000 flurocarbon film and the input SMA fitting. The sandwich is placed in a press at 200 psi and baked in an oven at 415 degrees F for 30 minutes. After removal from the oven, the unit must be allowed to cool before being removed from the press. The shorting screws are then added and the cavity joined to the assembly with nonmetallic screws. Conducting copper foil tape is placed around the cavity to prevent rf leakage that, were it to occur, would greatly modify the slot impedance.

An effort was made to optimize the design of the D-band slot. A single slot element was constructed in a stripline without the presence of the holes for the F-band elements. A transformer was incorporated into the center conductor to improve the match between the slot impedance and the impedance of the center conductor. The length of the quarter-wave cavity was reduced to 1.50 inches and the slot length was progressively reduced to 0.515 inch. These changes effectively reduced the VSWR. Figure 15 shows a partial three-band array sector using the element techniques described. The F-band slot was designed to operate at different frequency bands, depending upon the dielectric constant of the material used to fill the cavity.

---

*US Patent, 3,806,945, David Proctor, Stripline Antenna, 23 April 1974

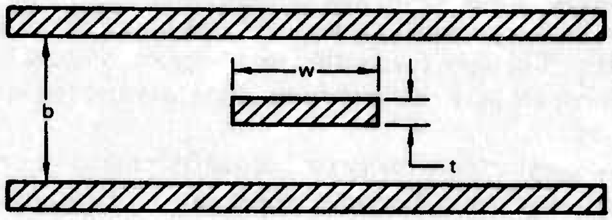

Figure 13. Stripline cross section.

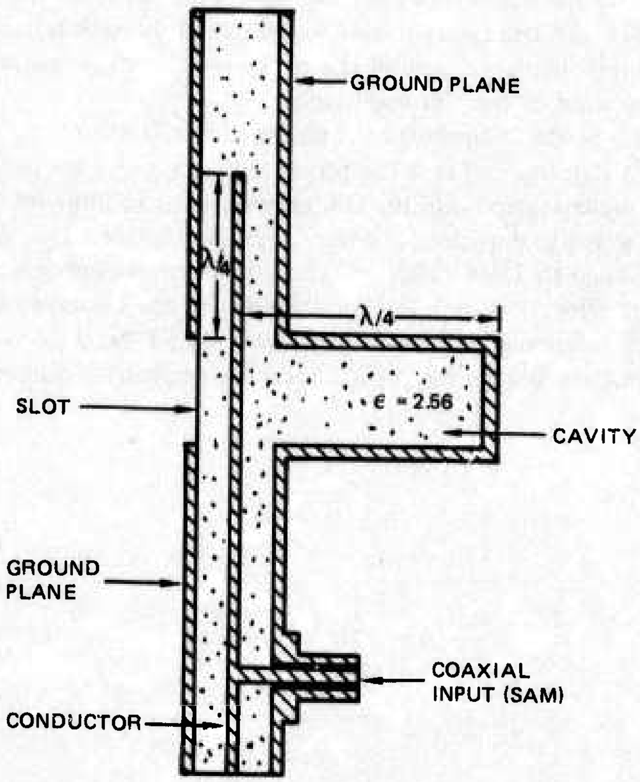

Figure 14. Typical D-band element cross section.

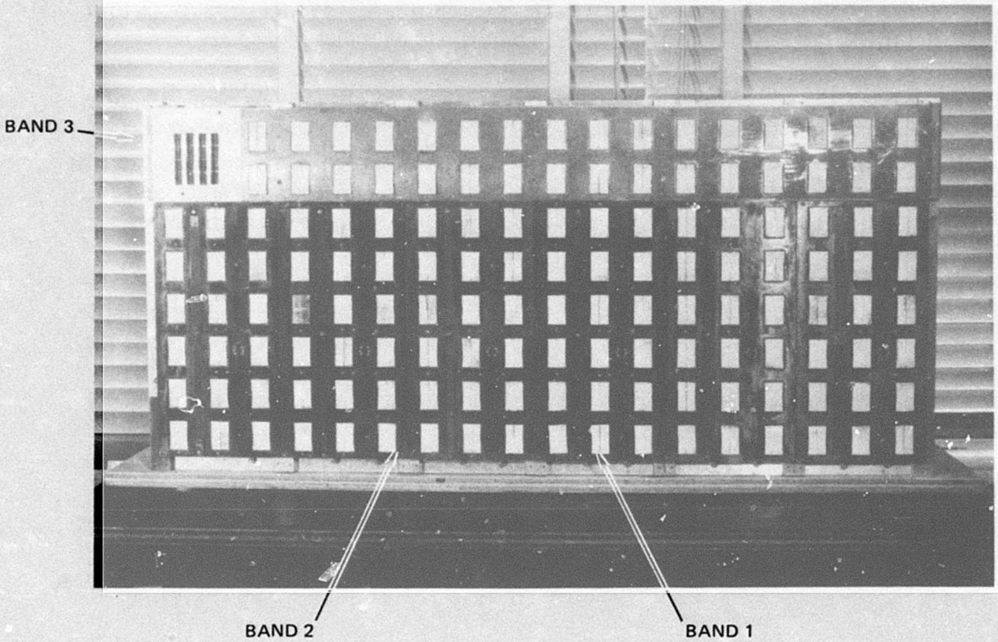

Figure 15. Three-band multifrequency array – stripline and cavity.

PART III

3.1 INTRODUCTION

Despite their numerous advantages, the rate of deployment of phased arrays into the Fleet has been disappointingly slow. The main reason given for this is that the initial investment cost of phased arrays is too high.

To take advantage of the unique capabilities of phased arrays, their cost must be reduced and to accomplish this, the available cost models must be studied to pinpoint the areas where the biggest cost savings can be made.

The initial investment cost for phased array hardware is divided into three cost constituents: (1) receiving components, (2) transmitting components, and (3) power producing components. These cost constituents are used to minimize the cost of a phased array system given the parameters of an attendant radar. They are further disaggregated into cost elements for which cost equations are available. Hence, the actual cost of the phased array system can be predicted.

Using the above complex cost model we now have the capability to measure the cost saving with new or novel phased array configurations.

3.2 FORMULATION OF INVESTMENT COST FOR THE HARDWARE FOR A PHASED ARRAY

The cost of the receiving components includes the cost of receiving elements, phase shifters, drivers, combiners, cables, power supplies for the phasors, and a prorated cost of the support structure. Similarly, the cost of the transmitting components includes the cost of phasors, transmitter modules, corporate feed, power supplies, harmonic filters, and the transmitting elements. The cost of the rf power components includes the high-power oscillators, amplifiers, cables, couplers, etc.

There are many different phased array antenna configurations and each configuration will have different costs included in each of the three constituent costs. For example, a space-fed array will have different cost components from a corporate-fed array since the space-fed array does not require the high power corporate feed. A phased array with a transmitter at every element will obviously have different cost components from an array with one high-powered transmitter and power dividers.

Some costs can be logically assigned on a prorated basis between different costs constituents. For example, if the receiving and transmitting elements are located on the same structure then the cost of the support structure can be divided between the receiving components and the transmitting components.

Thus, the total investment cost for the hardware of a phased array can be formulated as

$$C = C_r n_r + C_t n_t + C_p \bar{p} n_t \tag{27}$$

where

- C = investment cost of hardware for phased array
- C_r = the cost per element of the receiving components
- C_t = the cost per element of the transmitting components
- C_p = cost per element of components for producing rf power
- n_r = number of receiving elements
- n_t = number of transmitting elements
- $\bar{p}$ = average power radiated per element

The cost of a phased array for a radar is directly related to the figure of merit used for the radar. The figure of merit used for a tracking radar is different from that used for a search radar. Therefore, these two cases must be treated separately when relating cost to performance. The derivation given below relating cost to performance follows that published by L. J. Cantafio. [11]

3.2.1 SEARCH RADAR CASE

First consider the search radar case. The starting point is the familiar radar range equation

$$\left(\frac{2S}{N}\right)_o = \frac{2P_p G A_e \sigma}{(4\pi R^2)^2 k T_e B_n L} \tag{28}$$

or

$$\left(\frac{2S}{N}\right)_o = \frac{2P_p \tau G A_e \sigma}{(4\pi R^2)^2 k T_e L} \tag{29}$$

where

$\left(\frac{2S}{N}\right)_o$ = signal to noise ratio

P_p = peak power radiated

G = gain of the transmitting antenna

A_e = effective aperture of the receiving antenna

σ = radar cross section of target

R = maximum range of target

T_e = effective temperature

B_n = bandwidth

L = system loss

τ = pulse width

Various substitutions for variables in equation (29) are made so the relation between n_t, n_r and $\overline{p}$, and the performance parameters of the radar may be explicitly obtained.

In equation (29), the gain of the transmitting antenna G is given by

$$G = \eta_t \frac{4\pi}{\theta_B \Phi_B} \tag{30}$$

where

η_t = transmitting aperture efficiency,

θ_B, Φ_B = 3 dB beamwidth in the θ and Φ directions.

The effective receiving aperture, A_e is given by

$$A_e = \eta_r n_r d_x d_y \lambda^2 \tag{31}$$

where

η_r = receiving aperture efficiency

d_x, d_y = distance between receiving elements in the x and y directions.

The average power radiated, $\overline{P}$ is given by

$$\overline{P} = \eta_t n_t \overline{p} = P_p \tau \frac{\ell}{T}$$

or

$$P_p \tau = \eta_t n_t \overline{p} T/\ell \tag{32}$$

where

ℓ = number of pulses per period

T = period of waveform.

Assuming that the main beams of the phased array at the different phasor settings will crossover at the 3 dB levels

$$\theta_B \Phi_B = \theta/M \tag{33}$$

where

θ = search volume in steradians, and

M = number of beams required to search the volume.

The time required to search the prescribed volume is the frame time T_f. It is given by

$$T_f = MT/\ell \tag{34}$$

Substituting equations (30) through (34) into equation (29) and rearranging terms, one obtains

$$\overline{p} n_t n_r = \frac{2\pi R^4 k T_e L \, \theta \left(\frac{2S}{N}\right)_o}{\eta_t^2 \eta_r T_f d_x d_y \lambda \, \sigma} \tag{35}$$

The right side of this equation is a figure of merit for a radar in the search mode and is defined as W_s

$$\overline{p} n_t n_r = W_s \tag{36}$$

Using equation (36) and equation (27),

$$C = C_t n_t + C_r \frac{W_s}{\overline{p} n_t} + C_p \overline{p} n_t \tag{37}$$

Setting the derivative of C with respect to n_r equal to zero, an expression for the number of receiving elements which minimizes the total investment cost in hardware for a phased array can be formulated as follows:

$$(n_r)_{\text{min cost}} = \left[\frac{W_s\,(C_t + C_t\bar{p})}{\bar{p}C_r}\right]^{1/2} \tag{38}$$

Similarly, for the number of transmitting elements which minimizes cost we have

$$(n_t)_{\text{min cost}} = \left[\frac{C_r W_s}{\bar{p}(C_t + C_p\bar{p})}\right]^{1/2} \tag{39}$$

Equations (38) and (39) are utilized in equation (27) to formulate an expression for minimum cost

$$C_{\text{min}} = 2\left[\frac{C_r W_s}{\bar{p}}\,(C_t + C_p\bar{p})\right]^{1/2} \tag{40}$$

Using this equation we observe how the radar parameters affect the minimum cost of the phased array antenna.

A similar equation will now be derived for the minimum cost of a phased array for a track radar. Later the effect of the cost elements and radar parameters on the minimum cost will be examined.

3.2.2 TRACK RADAR CASE

A similar development is followed to derive an expression for a figure of merit for a radar in a tracking mode. Again, substitutions are made in the radar range equation to obtain an expression for $\bar{p}$, n_t, n_r in terms of the parameters of the tracking radar. Repeating the radar range equation

$$\left(\frac{2S}{N}\right) = \frac{P_p \tau G A_e\,\sigma}{(4\pi r^2)^2 k T_e L} \tag{29}$$

The expression now substituted for the gain G is

$$G = 4\pi\eta_t n_t d_x d_y \tag{41}$$

In the tracking mode the frame time is given by

$$T_f = N\frac{T}{\ell} \tag{42}$$

where

N = the maximum number for targets to be tracked.

The relation between the peak power radiated P_p and the average power radiated per element, $\bar{p}$ is the same as in the search mode case

$$P_p \tau = \eta_t n_t \bar{p}\ T/\ell$$

Using equation (16) and equation (6) we obtain

$$P_p \tau = \eta_t n_t \bar{p}\ \frac{T_f}{N} \tag{43}$$

As in the surveillance mode case, the effective aperture is given by

$$A_e = \eta_r n_r d_x d_y \lambda^2 \tag{31}$$

Thus, the radar range equation for the tracking mode can be put into the form

$$\left(\frac{2s}{N}\right)_0 = \frac{\bar{p}\eta_t^2 n_t^2 \eta_r n_r d_x^2 d_y^2 \lambda^2 \sigma T_f}{2\pi N R^4 k T_e L} \tag{44}$$

The standard deviation in tracking angle error in the θ direction has been shown [13] to be

$$\delta_\theta = \frac{\sqrt{3}}{\sqrt{\left(\frac{2s}{N}\right)_0}\ n_y d_y \pi} \tag{45}$$

Similarly, in the ϕ direction the standard deviation in angle tracking error is

$$\delta_\phi = \frac{\sqrt{3}}{\sqrt{\left(\frac{2S}{N}\right)_0}\ n_x d_x \pi} \tag{46}$$

where

n_x, n_y = number of elements in the x and y directions, respectively, and
$n_x n_y = n_r$

Multiplying equation (45) and equation (46) and rearranging terms we have

$$\left(\frac{2S}{N}\right)_0 = \frac{3}{\pi^2 \delta_\theta \delta_\phi n_r d_x d_y} \tag{47}$$

Substituting equation (47) into equation (44) we obtain an expression relating $\bar{p}$, n_t, n_r to the parameters of the radar in the tracking mode.

$$\bar{p}n_t^2 n_r^2 = \frac{6NR^4KT_eL}{\pi\delta_\theta\delta_\phi d_x^3 d_y^3 \lambda^2 \sigma T_f \eta_t^2 \eta_r} \tag{48}$$

The right side of equation (48) is a figure of merit for a radar in the track mode and is defined as W_t

$$\bar{p}n_t^2 n_r^2 = W_t \tag{49}$$

Equations (49) and (27) are used to obtain expressions for minimum cost in terms of the radar parameters. Substituting n_r from equation (49) into equation (27) we obtain

$$C = \left(\frac{W_t}{\bar{p}}\right)^{1/2} \frac{C_r}{n_t} + n_t\,(C_t + \bar{p}C_p)$$

Setting the derivative of C with respect to n_t equal to zero, we obtain an expression for the number of transmitters which minimizes the cost of the phased array antenna system

$$(n_t)_{\text{min cost}} = \left(\frac{W_t}{\bar{p}}\right)^{1/4} \left(\frac{C_r}{C_t \div C_p\bar{p}}\right)^{1/2} \tag{50}$$

In the same manner, we can substitute n_t from equation (49) into equation (27) to obtain

$$C = n_rC_r + \left(\frac{W_t}{\bar{p}}\right)^{1/2} \left(\frac{C_t + \bar{p}C_p}{n_r}\right)$$

Setting the derivative of C with respect to n_r equal to zero, we have

$$(n_r)_{\text{min cost}} = \left(\frac{W_t}{\bar{p}}\right)^{1/4} \left(\frac{C_t + C_p\bar{p}}{C_r}\right)^{1/2} \tag{51}$$

Using equations (50) and (51) in equation (27) we obtain

$$C_{min} = 2\left(\frac{W_t}{\bar{p}}\right)^{1/4} (C_r\,(C_t + C_p\bar{p}))^{1/2} \tag{52}$$

Thus, equations for the minimum cost for both the search and track radar cases have been formulated. Next the values for C_r, C_t and C_p must be found, then the effects of the radar parameters on the minimum cost can be examined.

3.3 COST MODEL FOR COST ELEMENTS

Once the minimum cost of a phased array as a function of the constituent costs has been derived, the best estimate of the constituent costs must be found. Because of its simplicity, accuracy, and generality, the cost model derived by B. C. Frederic [14] is used to obtain estimates of the constituent costs. This model uses the techniques of statistical cost correlation to derive cost equations for various cost elements as function of the radar parameters (frequency, peak power, etc).

Thus, for a typical high performance phased array radar, the cost constituents are divided into cost elements for which the cost equations are given. Each cost constituent will now be considered in turn.

The cost per element of the transmitting components, C_t, is disaggregated as follows:

$$C_t = C_{te} + C_{tcf} + C_{tps} + C_{tcm} \tag{53}$$

where

C_{te} = cost of transmitting element

C_{tcf} = cost of corporate feed

C_{tps} = cost of phase shifters

C_{tcm} = cost of calibration and monitoring

The cost equations utilized for each of these cost elements are given by Frederic [14].

The cost per element of the receiving components, C_r, is given by

$$C_r = C_{re} + C_{rcf} + C_{rps} + C_{rcm} + C_{pa} \tag{54}$$

where

C_{re} = cost of receiving element

C_{rcf} = cost of corporate feed

C_{rps} = cost of receive phase shifters

C_{rcm} = cost calibration and monitoring

C_{pa} = cost of preamplifiers

Cost equations for each of these five cost elements are given by Frederic [14].

Similarly, the cost per watt for rf power, C_p, is given by

$$C_p = C_{tm} + C_{ps} + C \tag{55}$$

where

C_{tm} = cost of transmitter modules

C_{ps} = cost of transmitter power supplies

C_{pcm} = cost of calibration and monitoring

3.4 SINGLE FREQUENCY CASE

Computer programs were created which used Frederic's cost equations together with equations (40) and (52) to calculate the minimum cost of a phased array antenna system for a high-performance radar. The radar was chosen to have phase-phase steering with a corporate feed and no switching between array faces. The chosen parameters were:

Signal to noise ratio, (2s/N)	10
Effective temperature, T_e	1500°K
Receiving aperture efficiency, η_r	80%
Transmitting aperture efficiency, η_t	55%
Frame time, T_f	1 second
Element spacing, $d_x = d_y$	0.6
Radar cross section of target, σ	$1m^2$

The variables and their ranges:

Loss, L	= 3 to 20dB
Range, R	= 100 to 500 km
Wavelength, λ	= .03 to 0.1 m
Number of targets tracked, N	= 10 to 100
Search volume, θ	= 1 to 12 steradians

The results of these computations are shown in figures 16 through 21.

From figure 16 it is seen that the minimum cost of a phased array for a search radar is increased by four when the range doubles. Thus, the minimum cost is proportional to the square of the range, whereas in the tracking radar case the minimum cost of the phased array is directly proportional to the range (fig 17).

In figure 18 the minimum cost of a phased array for a search radar is seen to be approximately proportional to the operating frequency. In other words, the minimum cost at L-band is 30% of the cost at S-band and only 10% of the cost at X-band. In a tracking radar the minimum cost of the phased array is approximately proportional to the square root of the rf frequency as shown in figure 19. Thus, the minimum cost of the phased array at L-band is 60% of the minimum cost at S-band and 30% of the minimum cost at X-band. It is obvious from a cost standpoint that it is better to construct search and track radar at the lowest allowable microwave frequency.

Figure 20 examines the minimum cost of the search radar phased array versus scan volume. In the search radar, the minimum cost of the phased array is approximately proportional to the square root of the search volume in steradians. Thus, the scan volume can be doubled for 40% increase in cost. Figure 21 shows the minimum cost of the track radar phased array and that it varies only as the fourth root of the number of targets. Therefore, to track fifty targets costs only 50% more than to track ten targets and a hundred targets can be tracked for a 78% increase in the cost to track ten targets. Thus, it is seen that large increases in the scan volume of number of targets can be achieved for a relatively small increase in cost.

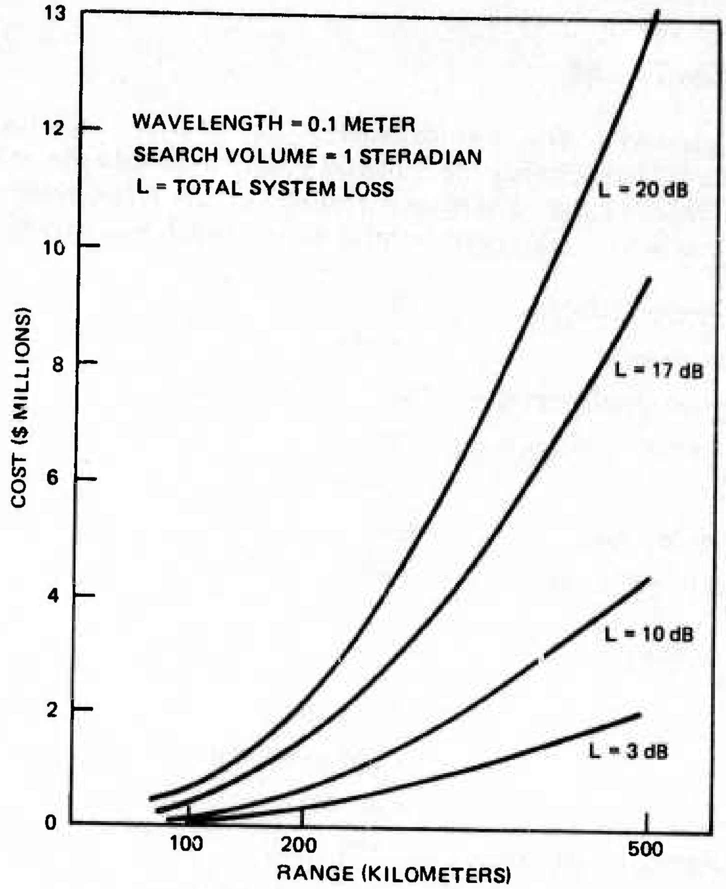

Figure 16. Cost of search radar versus range.

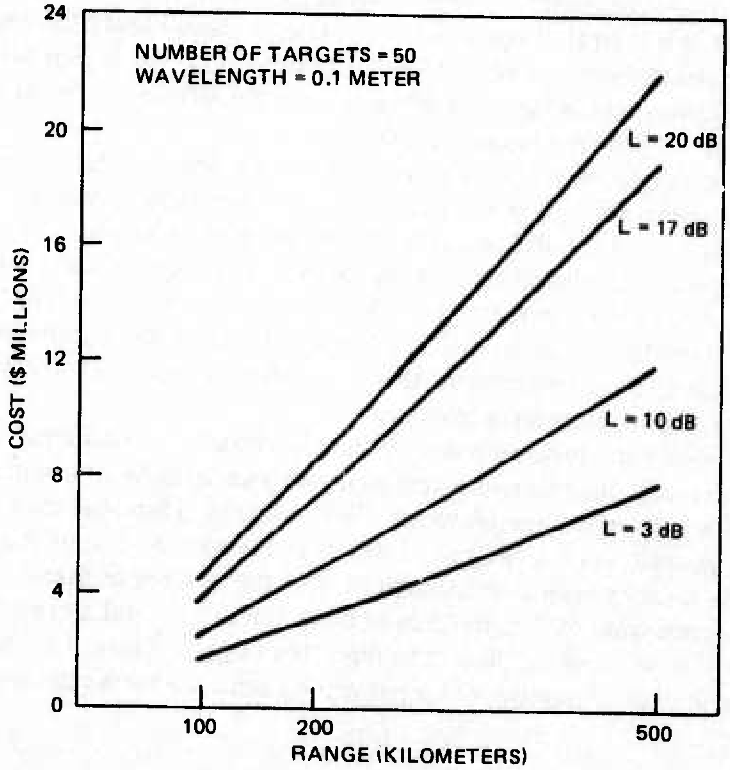

Figure 17. Cost of track radar versus range.

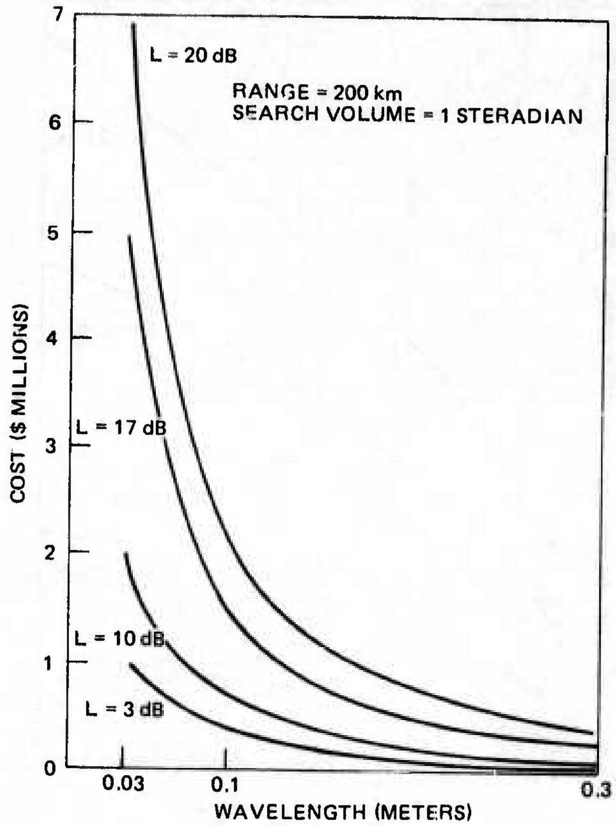

Figure 18. Cost of search radar versus wavelength.

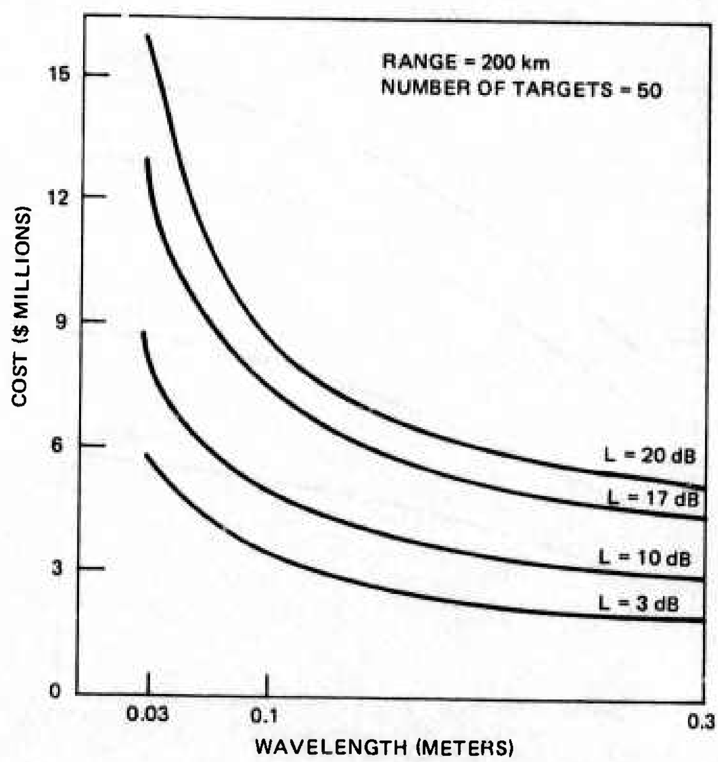

Figure 19. Cost of track radar versus wavelength

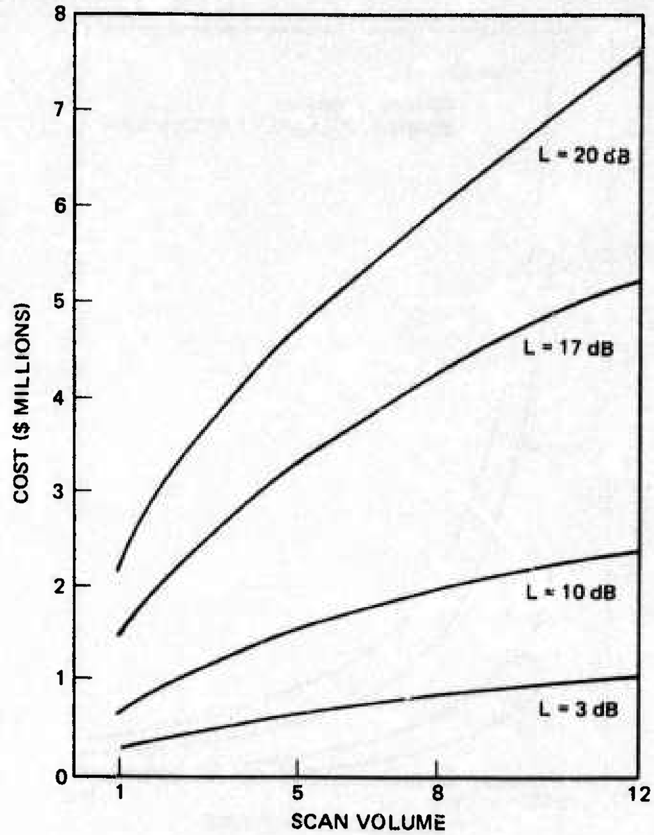

Figure 20. Cost of search radar versus scan angle.

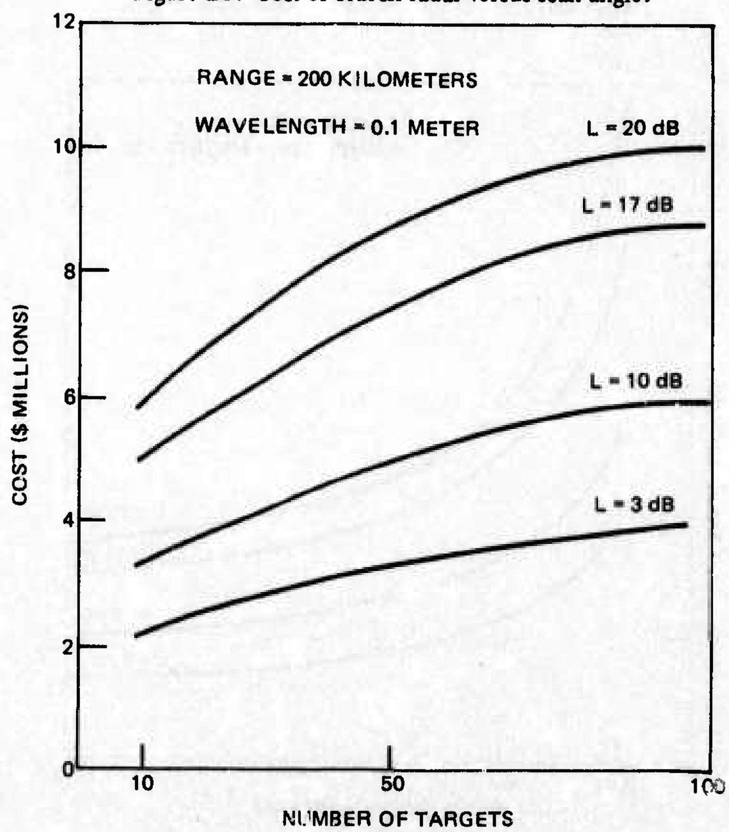

Figure 21. Cost of track radar versus number of targets.

In all of the cases considered here it is important to keep the loss of the total system at a minimum. A 3 dB increase in the losses in the search case increases the minimum cost by about 40%. In the tracking radar case the minimum cost of the phased array is increased by 20% if the losses are increased by 3 dB.

3.5 MULTIFREQUENCY CASE

To make significant progress in reducing the cost of phased arrays, novel design configurations must be examined. Using new cost models that have been developed, a measure of predicted cost savings of any new design configuration can be immediately obtained.

One configuration which is suggested is a multifrequency array that combines a search radar at 1 GHz with a tracking radar at 3 or 5 GHz. This concept makes use of phase shifters which are shared by the two frequency bands. If the phase increments are selected to be exact at one frequency but are also multiple at another, then the scanning process can be achieved at two frequencies. The beam pointing angle at each frequency need not be the same, and, in fact, it perhaps will not be. This concept, coupled with a two-band radiating element, could provide rapid scanning at two frequencies at a reduced cost.

A cursory look at the approach reveals that for a small number of elements, the concept is feasible. However, as the number of elements increases, the program for the phase shifters also increases to provide for beam agility. An additional benefit can accrue, since only one driver might be used to drive the phase shifter for both bands. The concept is shown schematically in figure 4. In some instances, it may be possible to use various bit phase shifters to obtain some beam positions. Extension of the approach to the three-band array is an obvious approach; whether the increase in complication would result in a commensurate increase in performance, while further reducing the cost, is an area for further investigation.

In this design the same phase shifters, radiating elements, and drivers are used by both radars. Thus, a significant savings can occur because the phasors and drivers are a major investment cost of any phased array system. The cost model was utilized to measure the cost of such a multifrequency, multifunction radar as compared to two separate radars performing the same functions.

The radar was assumed to use phase-phase steering with no switching between array faces. The chosen radar parameters are:

Signal to noise ratio, $(2S/N)_0$	10
Effective temperature, Te	1500 °K
Receiving aperture efficiency, ηr	80%
Transmitting aperture efficiency, ηt	55%
Frame time, T_f	1 second
Element spacing, dx = dy	0.6
Radar cross section, σ	$1 m^2$
Number of targets tracked	50
Search volume	1 steradian
Standard deviation of angle tracking error	10^{-3} radians

The results of the computer models shown in figure 22 give cost vs range for different system losses for both the multifrequency radar and the two single frequency radars. It is seen that substantial savings can occur by combining functions into one multifrequency radar which utilizes component commonality. Thus, at a range of 500 km and system losses of 20 dB, two separate radars cost 50% more than one multifrequency radar which performs the same functions. Actually, the cost saving ratio could be slightly less than 3:2 since more switching diodes could be required in a shared two-band driver/phase shifter than in a single one-band combination.

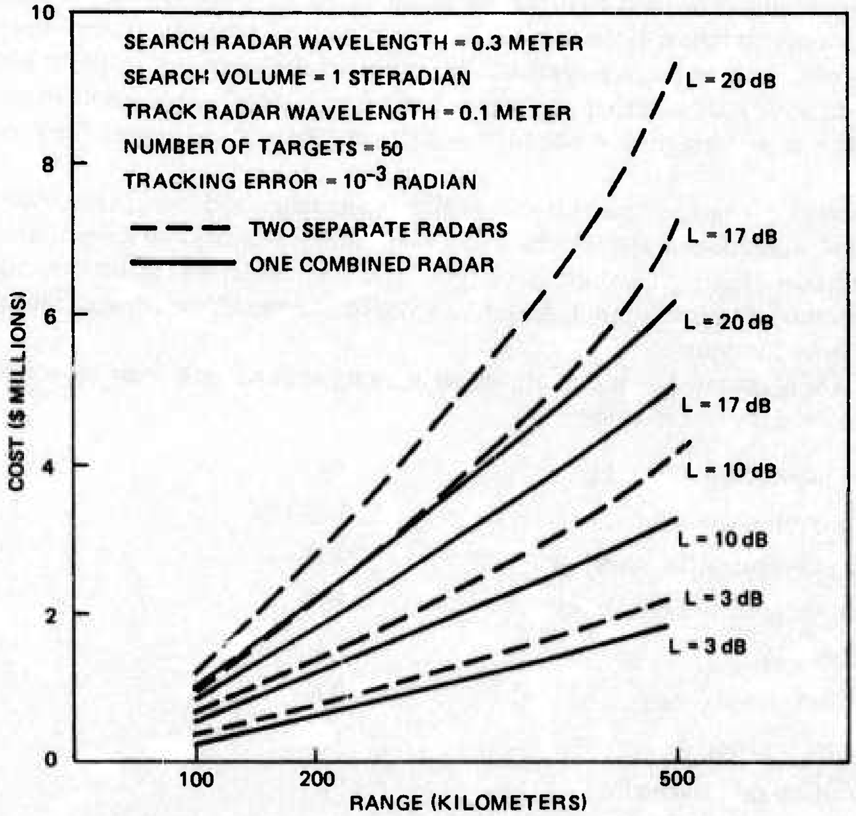

Figure 22. Cost of separate search and track radar phased arrays versus a multifrequency phased array.

PART IV

4.1 CONCLUSIONS

The use of array antennas has not been widespread and this has been due perhaps to their high cost. Also, there have been some misconceptions of the costs of these arrays when applied to small surface craft. In this context, the cost of the phased array may not be prohibitive since it can perform several functions at different frequency bands and therefore perform the tasks normally required of several radars. In addition, the use of some of the techniques described could provide low cost array antennas, as well as highly compact ones for application where physical space may be at a premium.

The concept of the multifrequency array could provide a cost-competitive antenna when commonality of components and lightweight techniques are used to replace several radar antennas. The concept of using a single phase shifter and radiating element to propagate several frequencies simultaneously needs further investigation in the area of mode coupling and examination of the impedance characteristics at the various frequency bands. In theory, for two frequencies which are even multiples of each other, the technique is feasible but the bandwidth properties have to be further explored.

The lightweight stripline techniques discussed have been used for large arrays at NELC. However, their potential for the smaller high-speed ships has not been exploited. This application requires a highly agile, rapidly scanning sector type of beam and that is a promising application especially when the benefits of MIC techniques can be used to exploit the space limitations, lightweight, and compactness of array antennas.

PART V

5.1 BIBLIOGRAPHY

1. Oliner, A. A., "The Radiation Conductance of a Series Slot in Strip Transmission Line," 1954 IRE Conv. Rec., vol 2, pt 8, p 89–90.

2. Manasse, R., "Maximum Angular Accuracy of Tracking a Radio Star by Lobe Comparison," IRE Trans. on Ant. and Prop., vol AP-8, p 50–56, Jan 1960.

3. MIT Lincoln Laboratories Report 299, Phased Array Radar Studies, 20 Feb 1963.

4. Jones, R. R. and Whicker, L. R., "A Digital Latching Ferrite Strip Transmission Line Phase Shifter," IEEE Transactions on Microwave Theory and Techniques, p 781, Nov 1965.

5. Cantofio, L. J., Prediction of the Minimum Cost of Phased Array Radar, Aerospace Corp. ATM-67 (s2925–35) –1, 1 Oct 1966.

6. Brown, J., Jr., Lavedan, L. J., Jr., Parks, J. K., Savage, B. R., "A Miniaturized C-Band Digital Latching Phase Shifter," IEEE Transactions on Microwave Theory and Techniques, p 688, Dec 1966.

7. Alverson, W. K., Pippin, J. E., Simon, J. W., "A Reciprocal TEM Latching Ferrite Phase Shifter," 1966 IEEE-GMTT International Symposium Digest, p 241.

8. Cheston, T. C., Frank, J., Querido, H., "Wide Band Phase Shifters," IEEE Transactions, AP-15, p 300, March 1967.

9. Frederic, B. C., A Predictive Cost Model for Phased Array Radars, General Research Corp., Santa Barbara, CA, Tech. Memo 492, Contract AF 04(694) – 934, June 1967.

10. Holtzman, J. C., "A Dual Band Array," IEEE Transactions, AP-16, p 603–604, Sept 1968.

11. White, J. F., "Review of Semiconductor Microwave Phase Shifters," Proc. IEEE, vol 56, p 1924–1931, Nov 1968.

12. Bell, C. V., Charlton, D. A., Grisword, R. E., Howard, R. W., Notvest, R. A., Stark, A., "Microwave Components for Wide-Band Phased Arrays," Proc. IEEE, vol 56, p 1908–1923, Nov 1968.

13. Boyd, C. R., Jr., Hord, W. E., Rosenbaum, F. J., "Applications of Reciprocal Latching Ferrite Phase Shifters to Lightweight Electronic Scanner Phased Arrays," Proc. IEEE, vol 56, p 1931–1939, Nov 1968.

14. Breithaupt, R. W., "Conductance Data for Offset Series Slots in Stripline," IEEE Transactions MTT-16, p 969–970, 1968.

15. Breithaupt, R. W. and Clarke, B., Two Fixed Beam Slotted Stripline Antenna Arrays, National Research Council of Canada, ERB-826, April 1969.

16. Astrahan, M. M. and Hughes, W. A., "The Duo-Mode Exciter," Proc. IRE, vol 37, p 1031, Sept 1969.

17. Naval Electronics Laboratory Center Report 1674, Interlacing of Multifrequency, Multifunction Integrated Arrays, by J. E. Boyns, 29 Dec 1969.

18. Naval Electronics Laboratory Center Report 1706, Multifrequency, Multifunction Integrated Arrays: Measurement Results, by J. E. Boyns, 21 April 1970.

19. Naval Electronics Laboratory Center Technical Note 1727*, Dual Beam Circular Array Study Experiment, by R. E. Parsley, 18 Aug 1970.

20. Temme, D. H., "Diode and Ferrite Technology," 1970 Phased-Array Antenna Symposium Proceedings, p 212–217, June 1970.

21. Hardeman, L. J., "Phased Arrays Scan Rapidly Towards Growth in the 70's," Microwaves, p 38, June 1970.

*NELC technical notes are informal publications intended primarily for use within the Center.

22. Arredondo, G. A., Butzien, P. E., and Humes, R. W., "The Design of a Wide Band Wide Scan-Angle Waveguide Radiating Element," 1970 Phased-Array Antenna Symposium Proceedings, p 173–177, June 1970.

23. Frank, J., "Bandwidth Criteria for Phased Array Antennas," 1970 Phased-Array Antenna Symposium Proceedings, p 243–253, June 1970.

24. Jones, W. R., Lee, S. W., Tang, R., Wong, N. S., "Multimode Phased Array Element for Wide Scan Angle Impedance Matching," 1970 Phased-Array Antenna Symposium Proceedings, p 178–186, June 1970.

25. Naval Electronics Laboratory Center Technical Report 1739, Microwave Integrated Circuits for Phase Arrays, by J. Reindel, 30 Oct 1970.

26. Saad, T., The Microwave Engineers' Technical and Buyers' Guide, p 30, 1970.

27. Naval Electronics Laboratory Center Technical Note 1839*, by J. E. Boyns and H. Valasek, 16 April 1971.

28. Boyns, J. E. and Provencher, J. H., Multi-Frequency Array Antennas, Proc. 1971 European Microwave Conference, Stockholm, Sweden, 23–28 Aug 1971.

29. Boyns, J. E. and Provencher, J. H., Multi-Frequency, Multi-Function Array Antennas, International Symposium on Antennas and Propagation, Sendai, Japan, 1–3 Sept 1971.

30. Adams, J. E., "Capability of a Projected 1975 Airborne Solid-State Phased-Array Radar," Microwave Journal, p 23, Sept 1971.

31. Boyns, J. E. and Provencher, J. H., "Experimental Results of a Multifrequency Array Antenna," IEEE Trans, Antennas and Propagation, vol AP-20, #1, Jan 1972.

32. Naval Electronics Laboratory Center Technical Report 1820, Multifrequency Antenna of Printed Dipoles, by J. E. Boyns and A. Munger, 18 Feb 1972.

33. Naval Electronics Laboratory Center Technical Document 155, Proc of the Array Antenna Conference, by J. E. Boyns and J. H. Provencher, 22–24 Feb 1972.

34. Naval Electronics Laboratory Center Technical Note 2008, Diode Phase Shifters and First Level Control Circuitry for a Cylindrical Array Radar Antenna, by P. Worcester, et al, 13 March 1972.

35. Naval Electronics Laboratory Center Technical Note 2037*, Some Aspects of Slot Design in Stripline for Array Antennas, by D. Proctor, 17 May 1972.

36. Naval Electronics Laboratory Center Technical Note 2047*, Lightweight Antenna Arrays for Small Craft, by J. H. Provencher and P. Worcester, 22 May 1972.

---

*NELC technical notes are informal publications intended primarily for use within the Center.

37. Naval Electronics Laboratory Center Technical Note 2058*, Lightweight Antenna for a Man-Pack Radar, by G. Vaughn and P. Worcester, 28 June 1972.

38. Naval Electronics Laboratory Center Technical Note 2060*, Three-Band Multifrequency Antenna, by D. Proctor, J. Boyns, P. Worcester, and H. Velasek, 24 July 1972.

39. Naval Electronics Laboratory Center Technical Report 1838, Microwave Integrated Circuits for Lightweight Array Antennas, by D. Rubin and P. Worcester, 21 Aug 1972.

40. Naval Electronics Laboratory Center Technical Report 1832, Microwave Integrated Circuits and Filter Design, by P. Worcester, 30 Oct 1972.

41. Byron, E. V., Cheston, T. C., and Laughlin, G. J., "Very Wide-Band Phased-Array Antenna," IEEE Transactions, AP-20, p 699–704, Nov 1972.

42. Fee, M. L., "Through Waveguide Dual-Frequency Antenna," IEEE Transactions, AP-20, p 781–784, Nov 1972.

43. Kummer, W. H., "The Properties of Half-Wave Slots in Two-Mode Rectangular Waveguide," IEEE Transactions, AP-21, p 202–206, March 1973.

44. Naval Electronics Laboratory Center Technical Note 2469*, Multi-Throw Microwave Diode Switches, by J. Reindel, 6 Sept 1973.

45. Muhuchy, W. and Scherer, G., "Wideband Phased Array Element With Rotatable Linear Polarization," 23rd USAF Antenna Symposium, Oct 1973.

*NELC technical notes are informal publications intended primarily for use within the Center.